Food Hydrocolloids 69 (2017) 422–431

Contents lists available at ScienceDirect

Food Hydrocolloids

journal homepage: www.elsevier.com/locate/foodhyd

Introduction and characterization of charged functional domains into an esterified pectic homogalacturonan by a citrus pectin methylesterase and comparison of its modes of action to other pectin methylesterase isozymes☆

Yang Kim [a, *], Martin A.K. Williams [b, c, d], Gary A. Luzio [e], Randall G. Cameron [e]

[a] Center for Food and Bioconvergence, Seoul National University, 1 Gwanakro, Gwanakgu, Seoul 08826, South Korea
[b] Institute of Fundamental Sciences, Massey University, Science Tower C4.09, Turitea Site, Palmerston North Campus, Private Bag 11222, Palmerston North 4442, New Zealand
[c] The Riddet Institute, Palmerston North, New Zealand
[d] The MacDiarmid Institute for Advanced Materials and Nanotechnology, New Zealand
[e] Citrus and Other Subtropical Products Research Unit, US Horticultural Research Laboratory, US Department of Agriculture, Agricultural Research Service, 2001 South Rock Road, Fort Pierce, FL 34945, USA

ARTICLE INFO

Article history:
Received 7 January 2017
Received in revised form
23 February 2017
Accepted 3 March 2017
Available online 6 March 2017

Keywords:
Pectin
Demthylesterified nanostructure
Citrus pectin methylesterase
Enzyme mode of action
Blockiness
Average block size

ABSTRACT

One of the four pectin methylesterase types isolated from *Citrus sinensis* var. Valencia fruit was used to demethylesterify a model homogalacturonan (HG) to 30%, 50% and 70% degree of methylesterification (DM) at pH 4.5 and 7.0, respectively. Introduced demethylesterified blocks (DMBs) were released by a *limited* endo-polygalacturonase (EPG) digestion, separated and quantified by HPAEC. Average DMB size ($\overline{BS}$) and number of such blocks per molecule ($\overline{BN}$) differed depending on final DM and reaction pH ($P < 0.05$). $\overline{BS}$ and $\overline{BN}$ were significantly higher in 30% DM HG than 50 and 70 DMs. pH 4.5 series showed significantly larger $\overline{BS}$ compared to pH 7.5 series ($P < 0.01$). Distribution of DMBs released by *limited* EPG digest was predicted by mathematical modeling and *in silico* modeled processive (degree of processivity = 10), multiple attack mode of action best explains the experimental block distributions. Absolute degree of blockiness (DB_{abs}) obtained from *exhaustive* EPG digestions, displayed a linear relationship with DM regardless of reaction pH ($P < 0.001$). Significant correlation coefficients between $\overline{BS}$, $\overline{BN}$, DB_{abs}, and DM manifested the effectiveness of the block information gained from both EPG digestion to estimate DMB distribution pattern ($P < 0.05$). However, comparison of block distribution information of three isozymes revealed that difference in block pattern could be manifested by parameters from *limited* EPG digest ($\overline{BS}$, $\overline{BN}$) but not by those from *exhaustive* digest (DB/DB_{abs}). The results suggested the possibility to control $\overline{BS}$ and to customize specific population of demethylesterified pectin molecules using PME isozymes from Valencia orange.

1. Introduction

Pectin is a natural substance found in plant cell walls and one of the most abundant polysaccharides on earth. However, its exact architecture, and complex chemical and macromolecular organization still need clarification. Galacturonic acid (GalA) is the main constituent of the three major pectic regions, homogalacturonan (HG), rhamnogalacturonan I and II (RG I and RG II). HG, the dominant pectic region, is a linear polymer of 1,4-linked α-D-galacturonic acid. RG I domain is made up of 4)- α -D-GalpA-(1,2)- α -L-Rhap-(1, repeats and may be further substituted with arabinans,

☆ This article is a US Government work and is in the public domain in the USA. Mention of a trademark or proprietary product is for identification only and does not imply a guarantee or warranty of the product by the US Department of Agriculture. The US Department of Agriculture prohibits discrimination in all its programs and activities on the basis of race, color, national origin, gender, religion, age, disability, political beliefs, sexual orientation, and marital or family status.

* Corresponding author. Center for Food and Bioconvergence, Seoul National University, Bldg203 # 409, 1 Gwanakro, Gwanakgu, Seoul 08826, South Korea.
E-mail addresses: ya_kim@hotmail.com (Y. Kim), m.williams@massey.ac.nz (M.A.K. Williams).

http://dx.doi.org/10.1016/j.foodhyd.2017.03.009
0268-005X/

galactans, and mixed arabinogalactans and are believed to be interspersed between HG domains linking multiple HG domains together (Coenen, Bakx, Verhoef, Schols, & Voragen, 2007; Yapo, Lerouge, Thibault, & Ralet, 2007). The most complex domain is RG II, which has a 1,4-linked α -D-GalA backbone that is substituted at defined positions with one of four possible oligosaccharides. To add to its complexity, the structure of pectin can be further modified through methylesterification at the C-6 position or O-acetylation at the C-2/C-3 position of GalA. (Ralet et al., 2008; Round, Rigby, MacDougall, & Morris, 2010; Thibault, Renard, Axelos, Roger, & Crepeau, 1993; Yapo et al., 2007).

The functionality of pectin is known to depend mostly upon the amount and distribution of unmethylesterified GalAs in the linear polymeric backbone. Recent investigations have revealed that distribution and size of contiguous unmethylesterified GalAs blocks have more importance than overall degree of methylesterification (DM) (Duvetter et al., 2009; Thibault et al., 1993; Van Buggenhout et al., 2006). Both the distribution and size of charged GalA blocks have been shown to affect the localized charge density of the HG region and its functionality related to forming complexes with β-lactoglobulin (Jones, Lesmes, Dubin, & McClements, 2010; Sperber, Schols, Cohen Stuart, Norde, & Voragen, 2009). The calcium dependent gelling functionality of pectin is mainly determined by the ability to form stable junction zones, hence it is critical to have the availability of unmethylesterified GalA blocks long enough for crosslinking via Ca^{2+} ion bridges (Braccini & Pérez, 2001). The minimum number of successive unmethylesterified GalA residues necessary to form a junction zone has been estimated to range from 6 to 20 (Braccini & Pérez, 2001; Luzio & Cameron, 2008). Pectin methylesterases (PMEs; EC 3.1.1.11) are utilized to introduce these ionic blocks of successive unmethylesterified GalA residues into an HG region which can serve as junction zones in many food, cosmetic, and pharmaceutical applications (Denes, Baron, Renard, Pean, & Drilleau, 2000; Hotchkiss et al., 2002). Among the PMEs, PMEs of plant origin mostly demethylesterify an HG region in a processive, blockwise mode thereby introducing charged domains into a single HG region (Denes et al., 2000; Duvetter et al., 2006; Fraeye et al., 2007; Kim et al., 2013, 2014). Several studies have been published on the differences in the mode of action of plant PME from different origins (Cameron, Luzio, Goodner, & Williams, 2008; Luzio & Cameron, 2008), for different isozymes within a single species (Savary, Hotchkiss, & Cameron, 2002), and even for a single isozyme at different pHs (Kim et al., 2014). Among them, isozymes exhibiting different modes of action within a single species are quite interesting since via reactions of PMEs with different mode of action, it will be enable pectin to be designed and tailored to possess specified functionality.

The presence of multiple forms of PME have been described from fruit tissue of citrus, tomato and grape fruit (Thibault et al., 1993; Willats et al., 2001; Hellin, Ralet, Bonnin, & Thibault, 2005; Louvet et al., 2006; Zega & D'Ovidio, 2016). Interestingly, only one of the four PME isozymes separated from sweet orange peel did not destabilize orange juice cloud while the other three PMEs destabilized the juice cloud at varying rates (Cameron, Baker, & Grohmann, 1998). One of the cloud destabilizing PMEs did not bind to the cation exchange matrix used in the separation of the multiple citrus PMEs at neutral pH (Cameron et al., 1998). Hence we have labelled it as a non-binding PME (NB-PME). Previous biochemical characterization of this enzyme revealed that two bands resolved by SDS-PAGE provided spectra common to citrus salt independent (SI-) PME (Savary, Vasu, Nunez, & Cameron, 2010). The pH-activity profiles in the presence and absence of 1.2% NaCl were also similar to those observed for SI-PME indicating this enzyme is also a salt-independent form thus suggested that this enzyme may be the translational product of this second homologous gene (Savary et al., 2010). Meanwhile, this enzyme caused the most rapid cloud loss at both 4 and 30 °C even though it is known to contribute only 6% of total PME activity in citrus fruit tissue (Cameron et al., 1998). These results suggested that the mode of action and/or physical and kinetic parameters of the different orange peel PME isozymes might vary. Previously, two of the four juice cloud destabilizing PMEs, SI-PME and thermally tolerant (TT-) PMEs, were characterized and their modes of action were investigated (Cameron et al., 2008; Cameron, Luzio, Vasu, Savary, & Williams, 2011). The mode of action modeled for the dominant SI-PME was consistent with a blockwise demethylesterification pattern at pH 7.5 (Cameron et al., 2008; Fraeye et al., 2007). However, the mode of action of TT-PME and consequent nanostructural modifications of pectin where quite different from those of the SI-PME and followed a simulated multiple-attack mechanism with a processivity of ~10 at both pH 7.5 and 4.5. The objectives of this study were to characterize the nanostructural features introduced during demethylesterification of a model homogalacturonan with the NB-PME from *Citrus sinensis* fruit tissue and to thereby elucidate its mode of action at pH 4.5 and 7.0. We present the results from both limited and exhaustive EPG digests, measuring non-methylesterified block distributions in order to characterize the pattern of charge distribution.

2. Materials and methods

2.1. Chemicals and reagents

All chemicals were purchased from Sigma–Aldrich (St. Louis, MO, USA) unless otherwise indicated. Aqueous buffer for the anion exchange chromatography mobile phase was composed of ammonium formate (no. 09735, >99% purity, Fluka BioChemika, Steinheim, Switzerland) in high purity deionized-distilled water. Endo-polygalacturonase (EPG) M2 was purchased from Megazyme International Limited (Bray, Ireland; lot 00304). Detailed methods for the production of monocomponent preparations of the non-binding NB-PME refer to Cameron et al. (1998).

2.2. Sugar composition

Pectin (91% methylesterified, from citrus fruit, Sigma-Aldrich, P9561) was prepared at a 1% concentration in 50 mM lithium acetate pH 4.5, 0.02% sodium azide, and digested with Rapidase ADEX-P (1 μL/mg pectin) for 24 h at 45 °C. The reaction was terminated by incubation at 70 °C for 10 min. Analysis of pectin soluble sugars was carried out using HPAEC-PAD as previously described (Widmer, 2011). Samples were filtered prior to injection with a 0.45 μm nylon syringe filter (Whatman, Kent, UK), and diluted 20-fold with deionized water so as to remain within the PAD detection limits. The separation gradient was altered slightly from the previous report of Widmer (2011): step two was lengthened by 2 min and the final concentration of 200 mM NaOH in step 4 was increased to 85%. No post-column eluent system was employed. Sugars were quantified via the external standard method, with 2-deoxy galactose as an internal standard (Chromquest V4, Thermo Fisher, Waltham, MA). The injection was performed in duplicate and the results averaged.

2.3. Demethylesterification

Pectin (91% methylesterified, from citrus fruit, Sigma-Aldrich, P9561) was made to a solution of 1% in 0.2 M LiCl. Purified NB-PME was added to 250 mL of the pectin solution at the level of 17.5 unit/g pectin at pH 7.0 or 35 unit/g pectin at pH 4.5, and the pH was maintained with a pH-stat controller (TIM856, Radiometer, France)

using 1 M LiOH as the titrant at 30 °C. A controlled demethylesterification series of 30%, 50% and 70% DM was produced at both pH values. When the desired DM had been reached the reaction was quenched by rapidly (~5 s) draining the reactor contents into a vessel containing two volumes of acidified 95% ethanol (pH 3.8) at 37 °C to precipitate the pectin and to halt the enzyme activity. The precipitated pectin was stored at 4 °C until centrifuged (23,400 g, 30 min, 4 °C) and the supernatant was discarded. The pellet was placed in liquid nitrogen, lyophilized and then ground to a fine powder. The pectin was stored at −80 °C until further analysis.

2.4. Molecular weight and DM of homogalacturonan

Size exclusion chromatography (SEC) was used to estimate weight average molecular weight (M_w), number average molecular weight (M_n) and DM using three inline detectors (Luzio & Cameron, 2008): a coupled contactless conductivity detector (Model C4D, eDAQ Inc., Colorado Springs, CO, hereafter referred to as a conductivity detector), multi-angle laser light scattering (MALLS; DAWN_ HELEOS, Wyatt Technologies, Santa Barbara, CA), and a differential refractive index (RI; Optilab DSP, Wyatt Technologies, Santa Barbara, CA) detector. Pectin samples were injected onto a set of three linear SEC columns (PL-aquagel-OH 50 and 60, Polymer Laboratories Inc., Amherst, MA and a TSK-GEL, TOSOHaas, Montgomeryville, PA) The columns were connected in series, enclosed in a column incubator, and kept at 27.0 ± 0.1 °C. The conductivity detector was equipped with a planar head stage (ET123) with contactless probes for ion chromatography/HPLC and was set at a gain setting of zero, amplitude of 100 V, and frequency of 500 kHz. Ammonium formate (100 mM) was used as mobile phase with flow rate of 0.6 mL/min. Samples were analyzed in duplicate.

2.5. Limited endo polygalacturonase digest

Demethylesterified pectins were dissolved at 0.25% (w/v) in 10 mL of 50 mM lithium acetate (pH 5.5), equilibrated at 30 °C in an incubator with stirring and digested with 50 μL of 1000 times diluted EPG M2 for 20 min. Preliminary EPG digests were performed to optimize the release of nonmethylesterified oligomers avoiding subsequent re-digestion by testing various EPG M2 amounts for various reaction times. Extended digests with EPG M2 resulted in the disappearance of larger oligomers and increased amounts of smaller oligomers, particularly GalA through $GalA_4$. EPG activity was quenched by pipetting 1 mL of the incubated solution into a beaker containing 7.5 μL of concentrated HCl to lower the pH to ~2, then microwaving the sample for 4 s to boiling, and finally immersing the sample in a boiling water bath for 10 min. The pH of digested samples was adjusted to ~5.5 with ammonium hydroxide after cooling to room temperature. For quantification of individual released oligomers, 100 μL or 200 μL of EPG digested samples were injected onto a CarboPac PA1 column (Cameron et al., 2008; Cameron et al., 2011; Kim et al., 2013) and eluted with an ammonium formate gradient (0–60 min, increasing from 0 to 60%, 60.1–180 min, from 60 to 80%, 180.1–195 min at 100%) in deionized water with a flow rate of 1 mL/min. Masses for each oligomer ($GalA_n$; where n is the number of demethylesterified GalA residues in the oligomer) were estimated using a pooled calibration curve constructed using $GalA_3$ (Sigma-Aldrich, St. Louis, MO, USA) and $GalA_8$ (purified from a partial EPG digest of polygalacturonic acid on a semi-preparative Carbo-Pac PA1 column). Oligomer mass estimates were converted to molar concentration as previously described (Cameron et al., 2008, 2011; Kim et al., 2013). Briefly, mass concentrations for each $GalA_n$ were used to calculate $GalA_n$ molar concentration per mL (C_n). The M_n for the parent pectin obtained from MALLS-SEC was used to estimate the molar concentration of pectin per mL (C_p). Eqs. (1)–(3) were used to estimate the average number of demethylesterified blocks of length n released from a molecule, the average sum of blocks per molecule ($\overline{B}$) and the average DMB size released ($\overline{BS}$), respectively. The number of average sized blocks per molecule was estimated according to Eq. (4).

$$\overline{B}_n = \frac{C_n}{C_p} \tag{1}$$

$$\overline{B} = \sum_{n=3}^{z} \overline{B}_n \tag{2}$$

$$\overline{BS} = \frac{\sum_{n=3}^{z} n\overline{B}_n}{\overline{B}} \tag{3}$$

$$\overline{BN} = \frac{\overline{B}}{\overline{BS}} \tag{4}$$

2.6. Mathematical modeling

For a detailed description related to the mathematical modeling refer to Cameron et al. (2008). Briefly, a set of chains is modeled as a set of simple one dimensional arrays of varying length and with the elements of each array representing nonmethylesterified GalA or methylesterified GalA in order to represent a hypothetical population of molecules. Here, the starting substrate for modeling was initiated as polygalacturonic acid and a random methylesterification algorithm was used to obtain the final DM. A number average DM of 94% and Degree of Polymerization (DP) of 140 were used for all simulations and up to 10^5 individual chains comprised the HG. A demethylesterification algorithm was run on the substrate until specified endpoints were achieved and the sample average DMs corresponded to those measured under the studied experimental conditions. By selecting the degree of multiple attack in the algorithm both random and processive modes of action could be investigated. Following the *in-silico* substrate modification the new intramolecular distribution of methyl esters was queried. The relative number (N) of different GalA block lengths M-$(G)_n$-M found in substrates demethylesterified to 30%, 50% or 70% assuming variable p values was returned by the simulation. Assuming that the endo-PG enzyme that then excises blocks from these M-$(G)_n$-M regions acts randomly within a DMB the relative probability of removing a k-mer from a block n long is given by:

$$P_{kn} = \frac{(n-2)-k+1}{\left((n-2)^2+(n-2)\right)/2} \tag{5}$$

In Equation (5), $n-2$ comes from the assumption that two unmethylesterified residues are needed in the EPG active site so whatever cuts are made an unmethylesterified residue is always left on either side (i.e. from a block of eight unmethylesterified residues an oligomer of six would be the largest extracted). With these approximations the relative probabilities (and consequent relative number of molecules) of the different DP oligomers predicted to be released by a limited EPG digest from substrates modified using PME models with various p values can be calculated. The simulation described above gives the relative numbers, N, of different GalA blocks of varied length, M-$(G)_n$-M, generated in the homogalacturonan and Equation (5) is then used to predict the relative number amount of different DP oligomers that would be released from contiguous blocks of a certain length. Merging the

approaches and summing the number of generated oligomers from each DMB weighted by the probability of occurrence of each initial contiguous stretch in the HG region the relative total number of GalA *k*-mers released (the experimentally determined quantity) is given by:

$$P_{oligo} = \sum_{n=k+2}^{n=chainlength} \frac{N(M-(G)_n-M)[(n-2)-k+1]}{\left\{\left[(n-2)^2+(n-2)\right]/2\right\}} \quad (6)$$

2.7. Degree of blockiness and absolute degree of blockiness using exhaustive EPG digest

Samples (0.25% w/v) in 0.05 mol L^{-1} lithium acetate (pH 5.5) were enzymatically digested with 5 U·mL^{-1} EPG M2 (Megazyme, Ireland) for 24 h and then denatured as previously described (Kim et al., 2014).

Quantification of GalA monomer, dimer and trimer in the EPG digested samples was accomplished by HPAEC using a Dionex CarboPac PA-1 anion exchange column (4 × 250 mm) coupled in-line behind a CarboPac PA-1 guard column (4 × 50 mm). A linear gradient of ammonium formate was used to produce calibration curves for monomeric, dimeric, and trimeric GalA, and for sample analysis (Kim et al., 2013). The injection volume for analysis of monomeric, dimeric, and trimeric GalA was 25–50 μL. Three replicate injections were performed for each injection volume, and the results averaged. Eluents were detected with an Evaporative Light Scattering Detector (ELSD-LT II; Shimadzu, Columbia, MD, USA) connected to house air (0% humidity, filtered to 0.01 mm) and pressurized to 4.5 Bar. Gain was set to 11 and drift tube temperature was set to 80 °C. Analyte peaks were observed and integrated using EZChrom Elite (Agilent Technologies, Santa Clara, CA). The DB and DBabs were calculated as follows:

$$DB = \left(\frac{M+D+T}{Free\ \ GalA}\right) \times 100 \quad (7)$$

$$DB_{abs} = \left(\frac{M+D+T}{Total\ \ GalA}\right) \times 100 \quad (8)$$

$$where\ \ (M+D+T) = \frac{ug^M}{MW^M} + \frac{ug^D}{MW^D} + \frac{ug^T}{MW^T} \quad (9)$$

$$Free\ \ GalA = \frac{(Q-Q(D))(G)(1-DM)}{Avg\ \ MW} \quad (10)$$

$$Total\ \ GalA = \frac{(Q-Q(D))(G)}{Avg\ \ \ MW} \quad (11)$$

$$Average\ MW = (176.14(1-DM)) + (190.18DM) \quad (12)$$

Q = μg of material injected; D = % water content; G = % GalA content; DM = degree of methylesterification; Avg MW = average molecular weight; M = monomer, D = dimer, T = trimer.

2.8. Statistical analysis

ANOVA and t-tests were carried out to examine the significance of DM and pH on the DMB parameters and DB obtained from limited and exhaustive digests. Multiple comparison tests were carried out using Tukey's HSD. Pearson's correlation coefficients were calculated to examine relationships between DB or DMB parameter and the rheology data. Regression analyses were carried out between DM, DB, DB_{abs}, and the concentrations of mono-, di- and tri-GalA released from complete EPG digests, using curve-fitting procedures available in SPSS 21.0. Analysis of Covariance (ANCOVA) was carried out with Graphpad Prism (version 4.03) to examine the difference of calibration curves derived with $GalA_3$ and $GalA_8$. All statistical tests were carried out at a significance level of 0.05 (95% confidence interval).

3. Results and discussion

3.1. Homogalacturonan and demethylesterified pectins

The parent pectin was composed of 90.1% GalA and 9% galactose indicating the parent pectin is a homogalacturonan. The weight average (M_w) and number average (M_n) molecular weights for the parent pectin were 67,440 Da and 36,510 Da, respectively, as determined by SEC-MALLS. Using the value for M_n, an average degree of polymerization (DP) of 194 was found for this HG which is somewhat higher than the range of 100–145 reported previously in the literature for HGs obtained from citrus pectins (Ralet et al., 2008; Thibault et al., 1993; Yapo et al., 2007). The calibration curve used to estimate M_n for this HG may have contained a broader molecular weight range than the reports referenced above, that could account for the increase in observed M_n and the resulting DP reported here. The DM of the parent HG was 90.8% as determined by SEC-C4D-MALLS-RI. M_w, M_n and the sugar composition of demethylesterified pectins did not exhibit significant difference when compared to the parent homogalacturonan.

3.2. Average demethylesterified block size and average number of blocks per molecule by limited EPG digest

GalA oligomers were released from all the demethylesterified pectins by limited digestions with EPG M2. $\overline{BS}$ of the DMBs released by the limited EPG digest might be an estimate of the actual DMBs present in the HG molecules and this is supported by the fact that the frequency of small oligomers did not increase with a decrease in DM, as might be predicted if high levels of secondary fragmentation occurred. ANOVA indicated significant differences among samples of different DMs for $\overline{B}$, $\overline{BS}$ and $\overline{BN}$ values for both pH series ($p < 0.05$; Table 1). Trends associated with decreasing DM values were similar for both pH series, with the sum of demethylesterified blocks ($\overline{B}$) and the length of blocks ($\overline{BS}$) increasing. Values reported here for average block lengths, $\overline{BS}$, are larger than those reported previously for citrus SI- and TT-PMEs (Table 2), and jelly fig *Fa*PME, yet, smaller than papaya *Cp*LPME with equivalent decreases in DM (Cameron

Table 1
Sum of DMB per molecule ($\overline{B}$), average DMB size ($\overline{BS}$) and number of average size DMB ($\overline{BN}$) per molecule.

	DM (%)	$\overline{B}$	*t*	$\overline{BS}$	*t*	$\overline{BN}$	*t*	DB (%)	*t*	DB_{abs} (%)	*t*
Parent	94	–		–		–		–		–	
pH 4.5	30	6.88^a	***	9.87^a	***	0.70^a	**	33.56^a		23.49^a	
	50	4.58^b	**	9.29^b	***	0.49^a	***	37.62^a		19.83^b	
	70	5.00^b	**	6.54^c	*	0.76^a	**	36.63^a		10.99^c	
pH 7.0	30	12.01^a		8.19^a		1.47^a		32.56^a		22.79^a	
	50	9.52^b		6.59^b		1.45^a		37.03^a		18.51^b	
	70	3.17^c		6.04^b		0.52^b		22.95^b	*	6.89^c	*

Values within a column that have different superscript letters indicate a significant difference ($P \leq 0.05$) based on ANOVA and Tukey's honestly significant difference test. All ANOVA models were significant at $P < 0.001$. Asterisks in column *t* indicate significant difference between means of pH pairs of each variable based on Student's *t*-test, *, ** and *** represent significant difference at $P < 0.05$, $P < 0.01$ and $P < 0.001$, respectively.

Table 2
Comparison of block structure of 50% DM HGs treated with isoforms of PME from Valencia orange.

50% DM	pH	$\overline{BS}$	$\overline{BN}$	Longest oligomer detected	DB (%)	DB_{abs} (%)
NB-PME	4.5	9.29	0.49	51	37.62	19.83
SI-PME[a]	4.5	8.9	3.6	50	–	–
TT-PME[b]	4.5	6.82	0.09	57	40.05	20.02
NB-PME	7.0	6.59	1.45	56	37.03	18.51
SI- PME[a]	7.5	–	–	47	–	–
TT-PME[b]	7.5	4.41	0.16	53	36.28	18.14

Values within a column that have different superscript letters indicate a significant difference ($P \leq 0.05$) based on ANOVA and Tukey's honestly significant difference test. All ANOVA models were significant at $P < 0.001$.
[a] $\overline{BS}$ and $\overline{BN}$ values were adopted from Cameron et al., 2008.
[b] $\overline{BS}$ and $\overline{BN}$ values were adopted from Cameron et al., 2011.

et al., 2008; Cameron et al., 2011; Kim et al., 2013, 2014). $\overline{BN}$ estimates decreased as $\overline{BS}$ increased in both pH series, repeating similar trends from our previous reports (Table 1) (Cameron et al., 2008; Cameron et al., 2011; Kim et al, 2013, 2014). Significant differences in $\overline{B}$, $\overline{BS}$ and $\overline{BN}$ between the two pH values were present at each DM ($p < 0.05$, Table 1). A similar trend was observed from citrus SI- and TT-PMEs (Cameron et al., 2008; Cameron et al., 2011), jelly fig *Fa*PME (Kim et al., 2014) and papaya *CpL*PME (Kim et al., 2013) and this suggested the possibility of customizing the block size and in advance, modulating the mode of action of PME via controlling treatment conditions.

3.3. Modeling of mode of action of NB-PME

Comparison of the experimentally and theoretically derived distributions of released oligomers from limited EPG digestions of demethylesterified HGs suggested a multiple attack mode of action for NB-PME (Fig. 1). The dotted, dashed and solid line in Fig. 1A–C shows distributions of oligogalacturonides predicted to be released by limited EPG digestions of HGs of 70, 50, and 30% DM, generated from a 94% DM starting substrate using either random demethylesterification or PME models as described above. The oligogalacturonide distributions produced from the NB-PME demethylesterified samples at pH 7.0 at all DM values investigated, conform to the simulated multiple-attack mechanism but additionally with a processivity (p) of around 10 giving good agreement of the predicted and experimental oligomers released by the limited digest. The 70% DM at pH 7.0 treatment produced DMBs of a very limited size ($DP \leq 20$) whereas pH 4.5 series produced DMBs up to $DP = 29$. It was observed that oligomers with a DP from 20 to 29 released from 70% DM pH 4.5 shifted towards a blockwise mode of action and this phenomenon was even more pronounced in 50% DM pH 4.5. For the 30% DM samples, results from both pHs were similarly fitted to a multiple attack mode of $p \leq 10$ with some deviation toward blockwise mode in DP range from ~20 to 30 in the pH 4.5 sample (Fig. 1C). Previous results of experimental curves of citrus SI-PME also showed a change of slope at around DP 20 with longer length fragments over DP 20 being better predicted by a single-chain mechanism while smaller fragments were fitted with $p = 1$ (Cameron et al., 2008).

A variable mode of action, dependent on the distribution of GalA C6 methyl esters on the HG region contained within the enzyme's active site, was previously proposed for several PMEs (Cameron et al., 2008; Cameron et al., 2011; Kim et al., 2013, 2014). Specifically, single chain blockwise mode of action was suggested for the citrus SI-PME within the range of DM from 50 to 80 (Cameron et al., 2008), $p = 10$ for citrus TT-PME (Cameron et al., 2011) and papaya PME (Kim et al., 2013) and multiple attack random mode of action

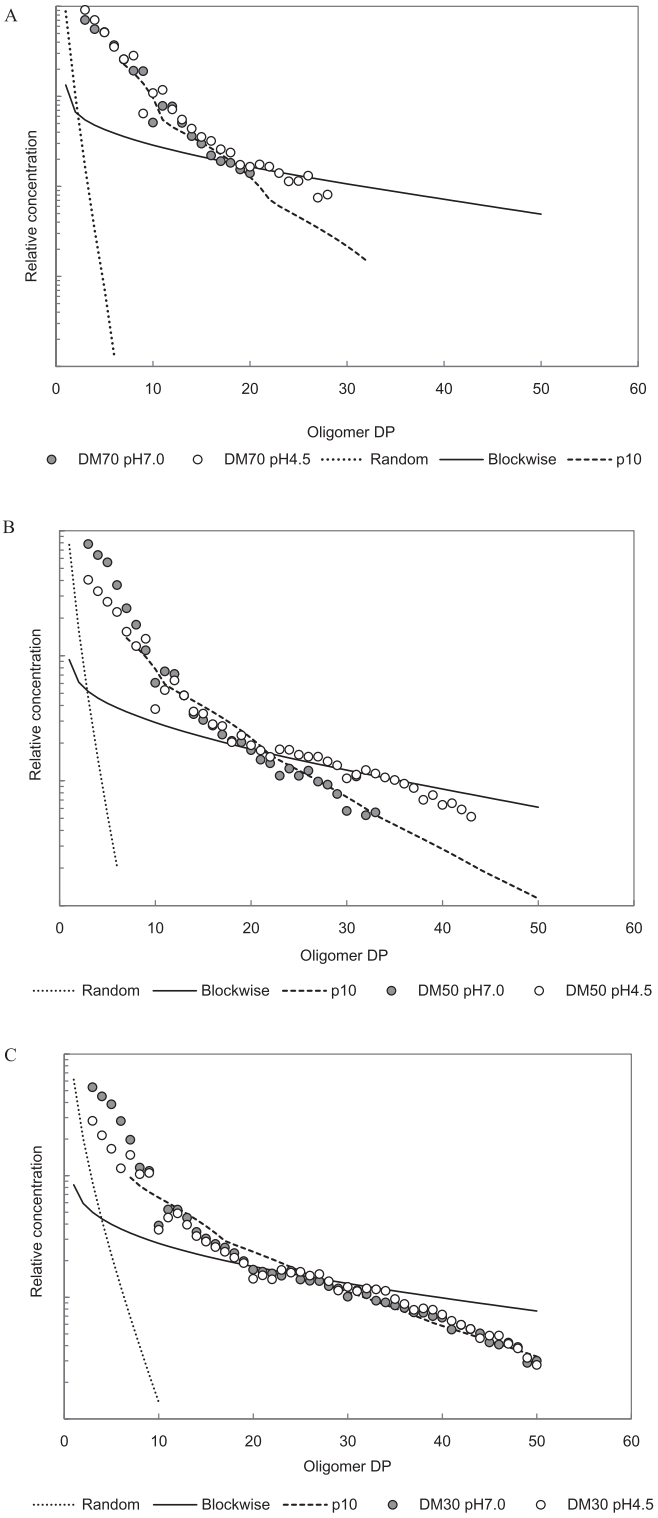

Fig. 1. Average E-$(G)_n$-E GalA oligomer distributions obtained by limited digestion with EPG from NB-PME demethylesterified pectins of 70% DM (A), 50% DM (B) and 30% DM (C) at pH 7.0 (closed) and pH 4.5 (open). Theoretical distribution lines for blockwise (single chain; solid line), p = 10 (multiple attack; dashed line) and random (multiple chain; dotted line) modes of action were obtained from *in-silico* modeling.

for jelly fig PME demethylesterified pectin of 70 DM (Kim et al., 2014). This could be supported by the previous study of Versteeg (1979) which reported a decrease in Km for pectins with decreasing DM (95.6–32.3%) for two citrus PMEs. An increase in the

affinity of the PMEs for their substrate associated with a reduction in DM supports the variably processive mode of action which we have presented here. It was also supported by recent studies of Mercadante, Melton, Jameson, & Williams (2013) and Mercadante, Melton, Jameson, Williams, & Simone (2014) which demonstrated *in silico* interactions between a processive *Erwinia* PME and HG decasaccharides. Their results proved that the substrate dynamics in PME binding groove are strongly influenced by the pattern of methylesterification of the HG chain, and also revealed that the ability to demethylesterify HG chains in processive way is tuned toward specific methylesterification patterns. Therefore, depending on the unique initial HG, demethylesterification pattern performed by each PME could be changed by the conformation of the substrate HG then that change also might affect the subsequent demethylesterification, resulting PME mode of action of blockwise or multiple attack with variable processivity.

3.4. Degree of blockiness and absolute degree of blockiness using exhaustive EPG digestion

The amount of mono-, di- and tri-GalAs released by exhaustive digestion with EPG increased linearly according to the decrease of DM, displaying high regression coefficients (R^2) of 0.933, 0.955 and 0.983 at pH 4.5 and 0.965, 0.959 and 0.971 at pH 7.0 (Fig. 2A and B). Linear relationships between DB_{abs} and the amount of each mono-, di- and tri-GalA released was also observed to display a regression with high R^2 of 0.996, 0.999 and 0.971 at pH 4.5 and 0.998, 0.996 and 0.937 at pH 7.0 (Fig. 2C and D). HG with 70% DM demethylesterified at pH 7.0 displayed significantly lower DB values than other HGs and no significant difference in DB values was observed among the other 5 samples. However, DB_{abs} values were significantly increased in accordance with a DM decrease in both pH series. In addition, a DB/DB_{abs} difference between pH pairs was only observed at 70% DM. The range of values for DB (22–37) and DB_{abs} (7–23) were obtained within DM range of 30–70% showing quite similar values for 50% DM previously obtained from citrus TT-PME from Valencia orange (Tables 1 and 2). However, DB and DB_{abs} values reported from demethylesterified pectins within a similar DM ranged from 90 to 95 and from 27 to 67, respectively (Ström et al., 2007), which were much higher than the DB/DB_{abs} reported in this study. Our DB/DB_{abs} values were also less than those reported from pectins treated with papaya PME (Kim et al., 2013) and jelly fig PME (Kim et al., 2014) within a similar DM range and rather similar to those obtained from base saponified or fungal PME demethylesterified pectins (Ngouémazong et al., 2011; Ström et al., 2007; Tanhatan-Nasseri, Crepeau, Thibault, & Ralet, 2011). From the definition of DB, the higher the DB of pectins at similar DM, the more blockwise the distribution of the methyl-esters in the pectin should be. However, there is a possibility that pectins having similar DM and DB values may still differ in the size of the blocks. According to EPG mode of action or its exhaustive digestion condition, 1 mol of tri-GalA release might be replaced by the release of 1 mol of each mono- and di-GalA, respectively, which could result in a two times increase of DB/DB_{abs} values compared to release as tri-GalA. Even though the amount of mono-, di-, tri-GalA linearly increases according to a DM decrease and a DB_{abs} increase, there could be still a difference of the slope of each linear regression between released mono-, di- and tri-GalA and DM manifesting that there could be some deviations for resulting DB/DB_{abs}. This difference might be characterized in future work by applying a secondary

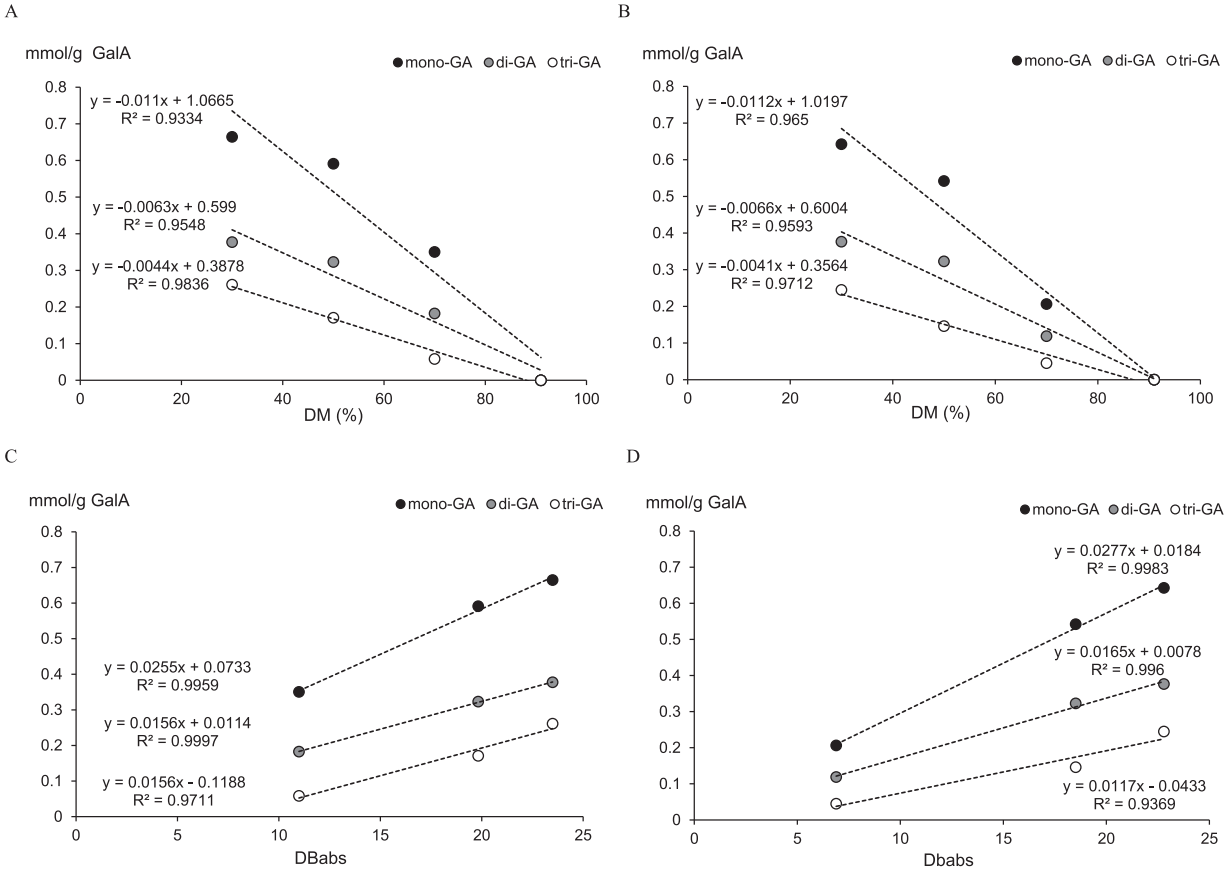

Fig. 2. Degree of blockiness (DB) and absolute degree of blockiness (DB_{abs}) as a function of the DM for both pH series of homogalacturonans. Open and close circles represent pH 7.0 series and pH 4.5 series, respectively.

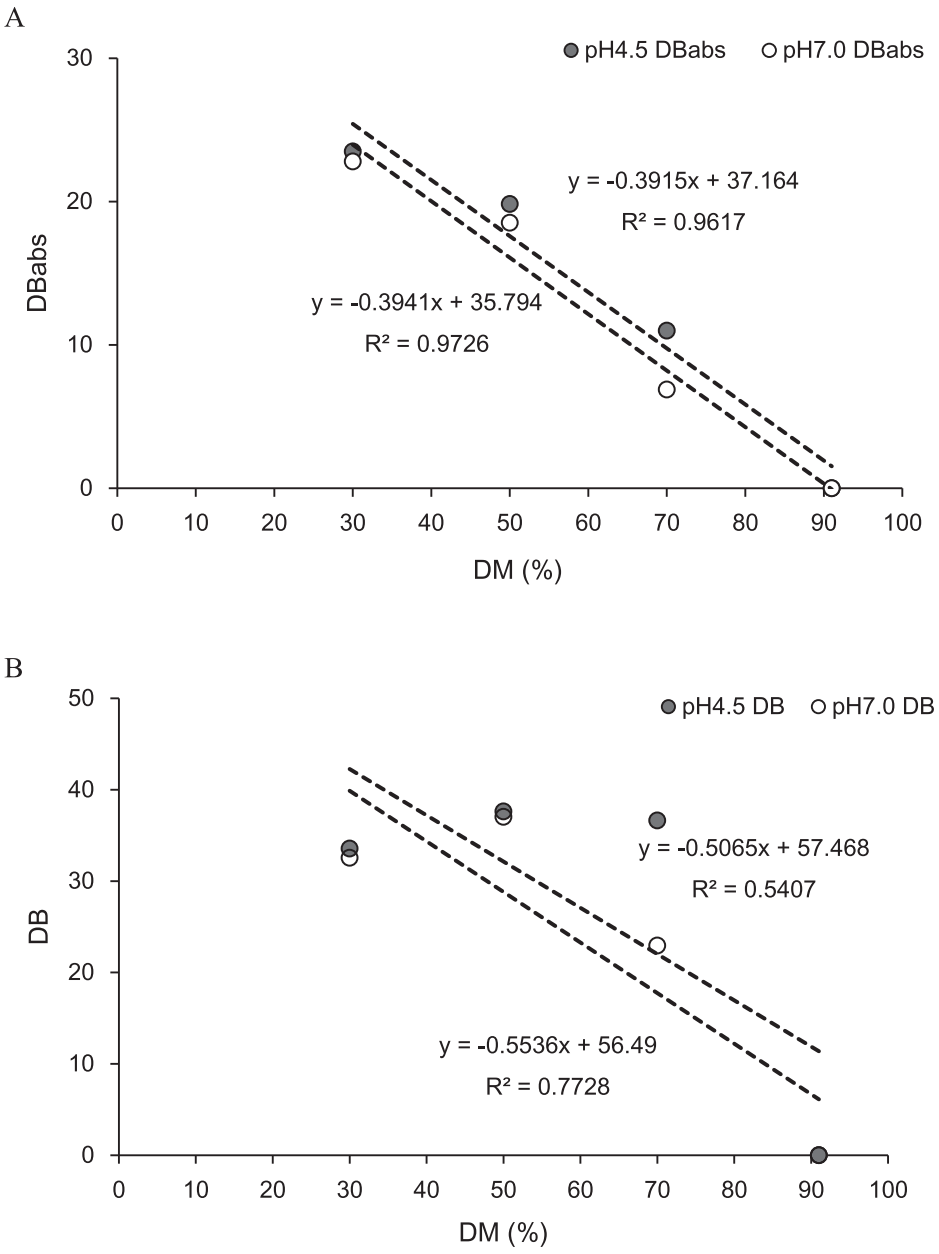

Fig. 3. Amount of mono-, di- and tri-GalA released upon endo-PG digest of demethylesterified pectins and their relationship with DM (A and B) and DB_{abs} (C and D). A and C pH 4.5, B and D pH 7.0.

Table 3
Pearson's correlation coefficient (r) representing the relationship between degree of methylesterification, degree of blockiness (DB), absolute degree of blockiness (DB_{abs}), sum of DMB per molecule ($\overline{B}$), average DMB size ($\overline{BS}$) and number of average size DMB ($\overline{BN}$) per molecule.[a]

	$\overline{BN}$	Mono-GalA	Di-GalA	Tri-GalA	DB	DB_{abs}	DM
$\overline{B}$	0.601*				−0.598*		
$\overline{BS}$	−0.830**	0.890**	0.902**	0.708*	0.790**	0.874**	−0.856**
$\overline{BN}$		−0.907**	−0.772**	−0.829**	−0.969**	−0.870**	0.777**
Mono-GalA			0.956**	0.950**	0.885**	0.996**	−0.965**
Di-GalA				0.889**	0.738**	0.973**	−0.987**
Tri-GalA					0.813**	0.959**	−0.933**
DB						0.845**	−0.732**
DB_{abs}							−0.982**

* and ** represent $P < 0.05$ and $P < 0.01$, respectively.
[a] Coefficients were calculated using pooled data of pH 4.5 and pH 7.0 series.

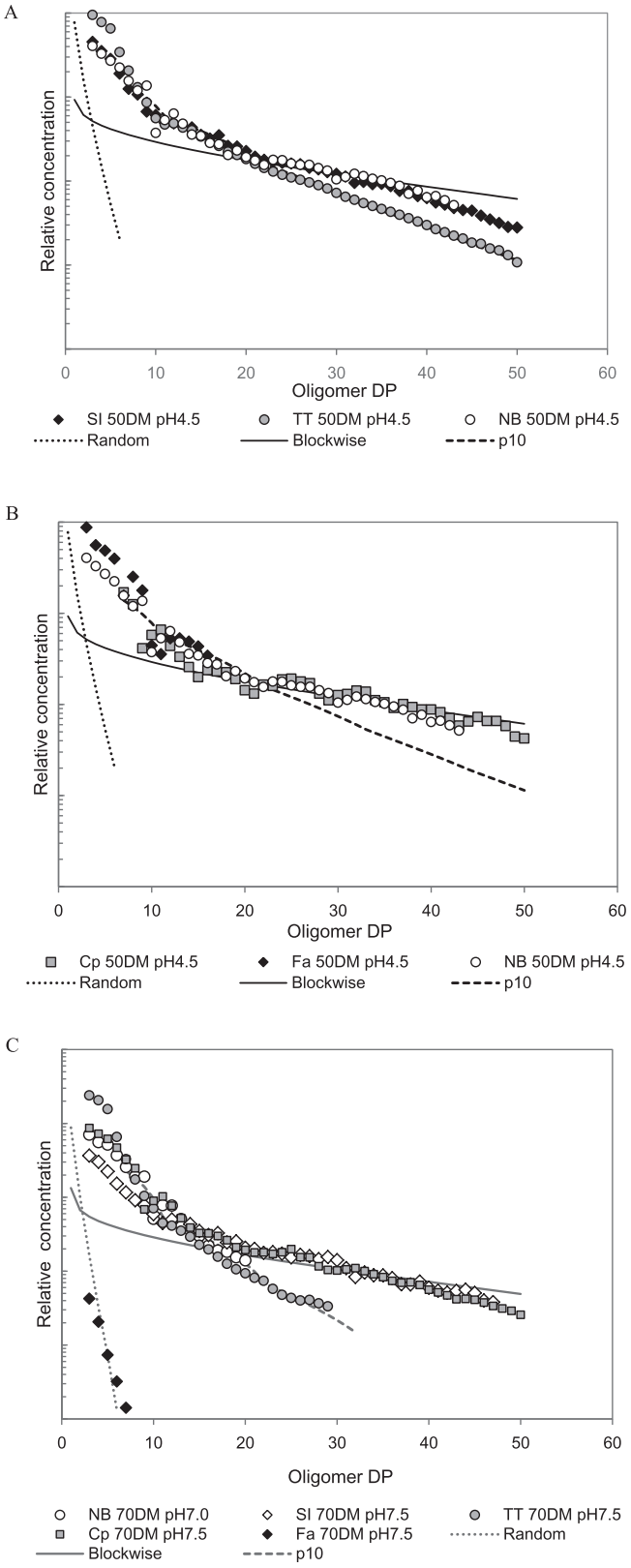

Fig. 4. Comparison of average M-(G)n-M GalA oligomer distributions obtained by limited digestion with EPG demethylesterified pectins using three PME isozymes, NB-PME (NB), salt independent PME (SI) and thermally tolerant PME (TT) from *Citrus sinensis* (A). Comparison of citrus PMEs, papaya Cp-PME from *Carica papaya*, jelly fig Fa-PME from *Ficus awkeotsang* Makino demethylesterified to 50% DM at pH 4.5 (B) and comparison of three citrus PMEs, Cp-PME, Fa-PME demethylesterified to 70% DM at pH 7.5 except for NB-PME at pH 7.0 (C). Theoretical distribution lines for blockwise (single chain), $p = 10$ (multiple attack) and random (multiple chain) modes of action were obtained from *in-silico* modeling. Average M-(G)n-M GalA oligomer distributions were adopted: SI-PME from Cameron et al., 2008; TT-PME from Cameron et al., 2011; Cp-PME from Kim et al., 2013; Fa-PME from Kim et al., 2014.

parameter to the calculation of DB and DB_{abs}, for example, the ratio of released mono-, di- and tri-GalA from the exhaustive EPG digests.

When the DB and DB_{abs} versus DM were plotted, DB_{abs} displayed a well-fitted linear regression with high R^2 of 0.962 at pH4.5 and 0.973 at pH7.0 but not the DB (Fig. 3A and B) which were observed from several previous studies on plant PMEs (Kim et al., 2013, 2014; Tanhatan-Nasseri, Crepeau, Thibault, & Ralet, 2011). Linear regression between DB_{abs} and DM displayed highR^2 for both pH 4.5 and pH 7.0 series within the tested DM range of ~30–91 (Table 2), even though the quadratic regressions improved the R^2 values for both pH series (pH 4.5: $y = -0.0042x^2 + 0.1122x + 24.058$, $R^2 = 0.998$; pH7.0: $y = -0.0013x^2 - 0.2394x + 31.767$, $R^2 = 0.976$). The relationship between these blockiness parameters and DM has been sought using demethylesterified pectin series with random, blockwise and various distributions of demethylesterified GalA residues (Daas, Meyer-Hansen, Schols, De Ruiter, & Voragen 1999; Daas, Voragen, & Schols, 2000; Guillotin et al., 2005; Ström et al., 2007; Ngouémazong et al., 2011; Tanhatan-Nasseri et al., 2011). Polynomial relationships between DB_{abs} and DM were reported in several series of random and block demethylesterified pectins in previous studies (Ngouémazong et al., 2011; Tanhatan-Nasseri et al., 2011). Ngouémazong et al. (2011) hypothesized that a perfect linear relationship between the DM and DB_{abs} of maximally blocky pectins, however, deviations with diverse degrees from linearity for DM vs. DB_{abs} might be also possible. Previously, linear relationships between DB_{abs} and DM were observed from exhaustive digestion using EPG M1 and M2 on jelly fig PME demethylesterified pectin with small blocks, and also observed from more blocky pectins demethylesterified by a papaya PME regardless of the demethylesterification pH (Kim et al., 2013, 2014). It is apparent that as the DM decreases demethylesterified blocks would merge and the block size would increase in a polynomial manner no matter what the initial demethylesterification patterns and distribution. This was demonstrated recently by Ralet et al. (2012) and is also implied by the low Y intercept of linear regressions between DM and DB_{abs} found at both pH series in current and previous studies (Kim et al., 2013, 2014).

3.5. Relationship between block parameters from exhaustive and limited EPG digestion of demethylesterified pectins

Highly significant coefficients (r) between DM, parameters from *exhaustive* EPG digest (amount of mono-GalA, di-GalA, tri-GalA, DB, DB_{abs}) and *limited* EPG digest ($\overline{B}$, $\overline{BS}$ and $\overline{BN}$) were demonstrated by Pearson's correlation from pooling the data of both pH series (Table 3). Positive correlations appeared between DB, DB_{abs} and $\overline{BS}$ ($P < 0.01$), accordingly, negative correlations were observed between DB, DB_{abs} and $\overline{BN}$ ($P < 0.01$). Negative correlation between $\overline{BS}$ and $\overline{BN}$ was based on the nature of these parameters since $\overline{BN}$ is defined as number of average sized blocks ($\overline{BS}$) per molecule thus when the sum of blocks is constant, average block size increases then $\overline{BN}$ decreases by definition (see equations presented in Methods section). Both DB and DB_{abs} also showed significant correlation with DM as shown in regression models (Fig. 3 and Table 3) and $\overline{BS}$ and $\overline{BN}$ also displayed highly significant correlation coefficient with DM ($P < 0.001$) verifying that the parameters from both complete and limited EPG digest gave consistent information related to the DM of pectins. The concentration of released mono-,

di-, and tri GalA also displayed high significant correlations with $\overline{BS}$ and $\overline{BN}$ which was obvious from the linear regression with DB_{abs} as well as DM presented in Fig. 2 and Table 3. High correlation between the block parameters demonstrated that the effectiveness of the techniques for the assessment of the fine structure of unmethylesterified GalA blocks introduced by NB-PME. It is worth note that previous reports of $\overline{BS}$ and DB_{abs} revealed high significant correlations with G′ of its calcium mediated gel verifying that the block distribution pattern is critical to determining the gelling properties (Kim et al., 2013, 2014). Accordingly, it would be possible to estimate the gelling properties by using these block parameters via mathematical modeling.

3.6. Comparison of block pattern introduced by PME isozymes from Valencia orange and their mode of actions

The demethylesterified block information of 50% DM samples estimated by both exhaustive and limited EPG digest of three PME isozymes, SI-PME, TT-PME and NB-PME from *Citrus sinensis* were presented in Table 2. All three isozymes displayed significant difference in $\overline{BS}$ and $\overline{BN}$ between pH conditions as well as among the isozymes at each pH condition. All three PMEs introduced a lower number of larger blocks at pH 4.5 compared to at pH 7.0 or 7.5. The longest oligogalacturonide observed from the PMEs were DPs around 50–57 displaying similarity among the isozymes, whereas the parameters from limited EPG digest represented huge difference among block parameters between the samples. DB (36–40) and DB_{abs} (18–20) from exhaustive EPG digest showed no significant differences demonstrating the incapability of these parameters to differentiate the block pattern introduced by different citrus PME isozymes from Valencia orange.

Fig. 4A and B shows the predictions for liberated GalA oligomers, as calculated by the summation method for DM 50% pectin samples demethylated assuming PME has a multiple-attack degree given by 1 (random), 10 or single-chain blockwise compared with experimental data obtained from 50 DM at pH 4.5. Fig. 4C shows these predictions and experimental data for demethylesterified pectins DM 70% at pH7.0 or 7.5. For TT-PME treated samples, the experimental data for DP > 7 seems qualitatively to best fit the form of those curves simulated assuming that the degree of multiple attack of the PME used is 10. In case of SI-PME, it was reported that the experimental curves showed change of slope or inflection at around DP 20 thus degree of multiple attack of around 1 at pH 4.5 or 10 at pH 7.5 were precedent, then the experimental data extended well above DP 20 clarifying that the relative frequencies of these longer length fragments are much better predicted by a single-chain mechanism (Cameron et al., 2008). The released oligogalacturonide distribution of *Carica papaya* PME treated pectins also displayed change of slope DP ~10 and also represented that the relative frequencies of longer length fragments are much better predicted by a single-chain mechanism, specifically for 50% DM pH 4.5 sample (Fig. 4B). That is, there are considerably higher amounts of these longer oligomers than would be predicted with a multiple-attack mechanism. Jelly fig 70% DM sample has the steepest slope among the tested samples observed suggesting that a pure multiple-attack mechanism ($p = 1$) (Fig. 4C).

In summary, three PME isozymes with different biochemical properties introduced various demethylesterified block size and numbers in a model homogalacturonan thus formally exhibiting that their differences related to juice cloud destabilization could be logically understood. These difference in block pattern could be clearly manifested by parameters from *limited* EPG digest results ($\overline{BS}$, $\overline{BN}$) but not by those from the exhaustive EPG digest (DB and DB_{abs}) despite of the high correlation of both parameters within the NB-PME series, revealing additional modifications or enhancements of the DB parameters are required to best explain the demethylesterified blocks within pectin molecules. The oligogalacturonide distributions produced from NB-PME demethylesterification conform to the simulated multiple-attack mechanism with a p of around 10 displaying good agreement of the predicted and experimental oligomers released by the limited digest. Some transition of mode of action was observed from pH 4.5 series for DP ~20–40 is not fully understood, but, one possible reason could be the difference of the starting DM between the HGs (~91) and the summation model (94). The well-characterized three citrus PMEs, SI-PME, TT-PME and NB-PME with distinctive demethylesterification properties might help improve the production of customized pectins and expand pectin's use for industrial applications.

Role of the funding source

This research was supported by a grant from USDA-NRI Program 71.1, Improving Food Quality and Value (#2009-35503-05205), the USDA, ARS Postdoctoral Research Associate Program–Class of 2011, the Basic Science Research Program through the National Research Foundation of Korea (NRF) funded by the Ministry of Science, ICT and Future Planning (No. NRF-2014R1A1A3052807) and USDA ARS CRIS 6618-41000-015–00D and USDA ARS CRIS 6618-41000-016–00D. These Funding Sources had no role in study design; in the collection, analysis, and interpretation of data; in the writing of the report; and in the decision to submit the paper for publication.

Acknowledgements

We would like to thank Peiling Li and Sandra Matlack for expert technical assistance; and Brett J. Savary for productive discussions and editorial assistance.

References

Braccini, I., & Pérez, S. (2001). Molecular basis of Ca (2+)-induced gelation in alginates and pectins: The egg-box model revisited. *Biomacromolecules, 2*(4), 1089–1096.

Cameron, R. G., Baker, R. A., & Grohmann, K. (1998). Multiple forms of pectin methylesterase from citrus peel and their effects on juice cloud stability. *J. Food Science, 63*, 253–256.

Cameron, R. G., Luzio, G. A., Goodner, K., & Williams, M. A. K. (2008). Demethylation of a model homogalacturonan with a salt-independent pectin methylesterase from citrus: I. Effect of pH on demethylated block size, block number and enzyme mode of action. *Carbohydrate Polymers, 71*(2), 287–299.

Cameron, R. G., Luzio, G. A., Vasu, P., Savary, B. J., & Williams, M. A. K. (2011). Enzymatic modification of a model homogalacturonan with the thermally tolerant pectin methylesterase from citrus: 1. Nanostructural characterization, enzyme mode of action, and effect of pH. *Journal of Agricultural and Food Chemistry, 59*(6), 2717–2724.

Coenen, G. J., Bakx, E. J., Verhoef, R. P., Schols, H. A., & Voragen, A. G. J. (2007). Identification of the connecting linkage between homo- or xylogalacturonan and rhamnogalacturonan type I. *Carbohydrate Polymers, 70*(2), 224–235.

Daas, P. J., Meyer-Hansen, K., Schols, H. A., De Ruiter, G. A., & Voragen, A. G. J. (1999). Investigation of the non-esterfied galacturonic acid distribution in pectin with endopolygalacturonase. *Carbohydrate Research, 318*, 135–145.

Daas, P. J., Voragen, A. G., & Schols, H. A. (2000). Characterization of non-esterified galacturonic acid sequences in pectin with endopolygalacturonase. *Carbohydrate Research, 326*(2), 120–129.

Denes, J. M., Baron, A., Renard, C. M., Pean, C., & Drilleau, J. F. (2000). Different action patterns for apple pectin methylesterase at pH 7.0 and 4.5. *Carbohydrate Research, 327*(4), 385–393.

Duvetter, T., Fraeye, I., Sila, D. N., Verlent, I., Smout, C., Hendrickx, M., et al. (2006). Mode of de-esterification of alkaline and acidic pectin methyl esterases at different pH conditions. *Journal of Agricultural Food Chemistry, 54*(20), 7825–7831.

Duvetter, T., Sila, D. N., Van Buggenhout, S., Jolie, R., Van Loey, A., & Hendrickx, M. (2009). Pectins in processed fruit and vegetables: Part I—stability and catalytic activity of pectinases. *Comprehensive Reviews in Food Science and Food Safety, 8*(2), 75–85.

Fraeye, I., De Roeck, A., Duvetter, T., Verlent, I., Hendrickx, M., & Van Loey, A. (2007). Influence of pectin properties and processing conditions on thermal pectin degradation. *Food Chemistry, 105*, 555–563.

Guillotin, S. E., Bakx, E. J., Boulenguer, P., Mazoyer, J., Schols, H. A., & Voragen, A. G. J. (2005). Populations having different GalA blocks characteristics are present in commercial pectins which are chemically similar but have different functionalities. *Carbohydrate Polymers, 60*(3), 391–398.

Hellin, P., Ralet, M.-C., Bonnin, E., & Thibault, J.-F. (2005). Homogalacturonans from lime pectins exhibit homogeneous charge density and molar mass distributions. *Carbohydrate Polymers, 60*, 307–317.

Hotchkiss, A. T., Savary, B. J., Cameron, R. G., Chau, H. K., Brouillette, J., Luzio, G. A., et al. (2002). Enzymatic modification of pectin to increase its calcium sensitivity while preserving its molecular weight. *Journal of Agricultural and Food Chemistry, 50*(10), 2931–2937.

Jones, O. G., Lesmes, U., Dubin, P., & McClements, D. J. (2010). Effect of polysaccharide charge on formation and properties of biopolymer nanoparticles created by heat treatment of β-lactoglobulin–pectin complexes. *Food Hydrocolloids, 24*(4), 374–383.

Kim, Y., Williams, M. A. K., Galant, A. L., Luzio, G. A., Savary, B. J., Vasu, P., et al. (2013). Nanostructural modification of a model homogalacturonan with a novel pectin methylesterase: Effects of pH on nanostructure, enzyme mode of action and substrate functionality. *Food Hydrocolloids, 33*(1), 132–141.

Kim, Y., Williams, M. A. K., Tzen, J. T. C., Luzio, G. A., Galant, A. L., & Cameron, R. G. (2014). Characterization of charged functional domains introduced into a modified pectic homogalacturonan by an acidic plant pectin methylesterase (Ficus awkeotsang Makino) and modeling of enzyme mode of action. *Food Hydrocolloids, 39*(0), 319–329.

Louvet, R., Cavel, E., Gutierrez, L., Guenin, S., Roger, D., Gillet, F., et al. (2006). Comprehensive expression profiling of the pectin methylesterase gene family during silique development in Arabidopsis thaliana. *Planta, 224*, 782–791.

Luzio, G. A., & Cameron, R. G. (2008). Demethylation of a model homogalacturonan with the salt-independent pectin methylesterase from citrus: II. Structure function analysis. *Carbohydrate Polymers, 71*, 300–309.

Mercadante, D., Melton, L. D., Jameson, G. B., & Williams, M. A. K. (2014). Processive pectin methylesterases: The role of electrostatic potential, breathing motions and bond cleavage in the rectification of Brownian motions. *PLoS ONE, 9*, e87581.

Mercadante, D., Melton, L. D., Jameson, G. B., Williams, M. A. K., & Simone, A. D. (2013). Substrate dynamics in enzyme action: Rotations of monosaccharide subunits in the binding groove are essential for pectin methylesterase processivity. *Biophysics Journal, 104*, 1731–1739.

Ngouémazong, D. E., Tengweh, F. F., Duvetter, T., Fraeye, I., Van Loey, A., Moldenaers, P., et al. (2011). Quantifying structural characteristics of partially de-esterified pectins. *Food Hydrocolloids, 25*(3), 434–443.

Ralet, M. C., Crepeau, M. J., Lefebvre, J., Mouille, G., Hofte, H., & Thibault, J. F. (2008). Reduced number of homogalacturonan domains in pectins of an Arabidopsis mutant enhances the flexibility of the polymer. *Biomacromolecules, 9*(5), 1454–1460.

Ralet, M. C., Williams, M. A. K., Tanhatan-Nasseri, A., Ropartz, D., Quéméner, B., & Bonnin, E. (2012). Innovative enzymatic approach to resolve homogalacturonans based on their methylesterification pattern. *Biomacromolecules, 13*(5), 1615–1624.

Round, A. N., Rigby, N. M., MacDougall, A. J., & Morris, V. J. (2010). A new view of pectin structure revealed by acid hydrolysis and atomic force microscopy. *Carbohydrate Research, 345*(4), 487–497.

Savary, B. J., Hotchkiss, A. T., & Cameron, R. G. (2002). Characterization of a salt-independent pectin methylesterase purified from Valencia orange peel. *Journal of Agricultural and Food Chemistry, 50*, 3553–3558.

Savary, B. J., Vasu, P., Nunez, A., & Cameron, R. G. (2010). Identification of thermolabile pectin methylesterases from sweet orange fruit by peptide mass fingerprinting. *Journal of Agricultural and Food Chemistry, 58*, 12462–12468.

Sperber, B. L. H. M., Schols, H. A., Cohen Stuart, M. A., Norde, W., & Voragen, A. G. J. (2009). Influence of the overall charge and local charge density of pectin on the complex formation between pectin and β-lactoglobulin. *Food Hydrocolloids, 23*(3), 765–772.

Ström, A., Ribelles, P., Lundin, L., Norton, I. T., Morris, E. R., & Williams, M. A. K. (2007). Influence of pectin fine structure on the mechanical properties of calcium–pectin and acid–pectin gels. *Biomacromolecules, 8*(9), 2668–2674.

Tanhatan-Nasseri, A., Crepeau, M. J., Thibault, J. F., & Ralet, M. C. (2011). Isolation and characterization of model homogalacturonans of tailored methylesterification patterns. *Carbohydrate Polymers, 86*(3), 1236–1243.

Thibault, J. F., Renard, C. M. G. C., Axelos, M. A. V., Roger, P., & Crepeau, M. J. (1993). Studies of the length of homogalacturonic regions in pectins by acid hydrolysis. *Carbohydrate Research, 238*(4), 271–286.

Van Buggenhout, S., Messagie, I., Maes, V., Duvetter, T., Van Loey, A., & Hendrickx, M. (2006). Minimizing texture loss of frozen strawberries: Effect of infusion with pectinmethylesterase and calcium combined with different freezing conditions and effect of subsequent storage/thawing conditions. *European Food Research and Technology, 223*(3), 395–404.

Versteeg, C. (1979). *Pectinesterases from the orange: Their purification, general characteristics and juice cloud destabilizing properties*. Wageningen, The Netherlands.: Agricultural University (Ph.D).

Widmer, W. (2011). Analysis of biomass sugars and galacturonic acid by gradient anion exchange chromatography and pulsed amperometric detection without post-column addition. *Biotechnology Letters, 33*, 365–368.

Willats, W. G., Orfila, C., Limberg, G., Buchholt, H. C., van Alebeek, G. J., Voragen, A. G., et al. (2001). Modulation of the degree and pattern of methylesterification of pectic homogalacturonan in plant cell walls. Implications for pectin methyl esterase action, matrix properties, and cell adhesion. *Journal of Biological Chemistry, 276*, 19404–19413.

Yapo, B. M., Lerouge, P., Thibault, J.-F., & Ralet, M.-C. (2007). Pectins from citrus peel cell walls contain homogalacturonans homogeneous with respect to molar mass, rhamnogalacturonan I and rhamnogalacturonan II. *Carbohydrate Polymers, 69*, 426–435.

Zega, A., & D'Ovidio, R. (2016). Genome-wide characterization of pectin methyl esterase genes reveals members differentially expressed in tolerant and susceptible wheats in response to Fusarium graminearum. *Plant Physiology and Biochemistry, 108*, 1–11.